

# Hybrid Method for Training Customized CNN mode for Pomegranate Disease Detection, Classification and Control Mechanisms

Naheeda Tharannum B.<sup>1\*</sup> and Venkateshappa<sup>2</sup>

<sup>\*1</sup>Research Scholar, School of ECE, REVA University, Bangalore, Karnataka, India

<sup>\*1</sup>Assistant Professor, Government Engineering College, Raichur, Karnataka, India

<sup>2</sup>Professor, School of ECE, REVA University, Bangalore, Karnataka, India

**\*Corresponding Authors Email ID: [naheeda.rcr@gmail.com](mailto:naheeda.rcr@gmail.com)**

---

## ARTICLE INFO

## ABSTRACT

Received: 20 Dec 2024

Revised: 15 Feb 2025

Accepted: 25 Feb 2025

fruit is both a medicinal and fruit plant cultivated in large quantity in Karnataka. Diseases are the main reasons that impact post-harvest profit and production. Identifying the diseases through automated methods by using real time images will provide information on control mechanisms for farmers. Detecting the diseases on field with simple mobile apps that are loaded on the farmers mobile that connect to background network for data access and inference of disease is an important step to reduce production loss and recommend control mechanisms for spread of disease. In this work, new methods are proposed that combines wavelet features, support vectors, customized CNN model (TinyYOLOV4) and control mechanisms that provide quick information to the farmer once the photograph is uploaded in the app. The classification accuracy of the proposed model is 99.4% and is generates the inferences faster that aids real time assistance. Two methods are combined to provide control mechanism and to improve mean average precisions. The model is validated and demonstrates 4% improvement in precision accuracy compared with existing methods.

**Keywords:** Discrete Wavelet Transform, Pomegranate Disease, CNN, Tiny Yolo, Support Vectors, Control mechanisms, Classification

---

## 1. Introduction

Pomegranate is a most liked fruit by all people as it contains ellagitannins, which are bioactive polyphenols, chemical compounds that is found in both the peel and the seeds and induces anti-inflammatory effects on cells in the body. When pomegranate is consumed and it ferments into urolithins, that when absorbed by the body is an anti-ageing substance halting inflammation and improves cardiac functioning [1]. It contains Vitamin C, fibre, manganese, folate and thiamine that helps body fight many diseases. The global market is 8.46 billion USD by 2026 [2] and in India pomegranate is cultivated in Maharashtra, Karnataka and Andhra Pradesh. Most of the pomegranate cultivate in India is exported to major countries like UAE, UK and Bangladesh as per the reports published in National Horticulture Board [3]. The districts of Bijapur, Bagalkot, Koppal, Bellary, Belgaum, and Chitradurga are the major pomegranate growing regions in the state. Ganesh, Mridula (Arakta), Ruby, Bhagwa (Kesar), Jyoti, and Super Bhagwa are the varies types of pomegranate crop grown in Karnataka. Total area in Karnataka for pomegranate is 25.69 ('000 Ha) with production of 255.01 ('000 MT). From Karnataka the total export of pomegranate reached 33.5 million USD and is expected to reach 65 million USD by 2026. The common diseases in pomegranate fruit are: Bacterial blight, anthracnose, aspergillus fruit rot, fruit cracking, root rot, aphids, alternaria black spot, grey mold rot, wilt and green mold. Diseases that infect pomegranate post-harvest are Botrytis cinerea, Alternaria alternata, Penicillium implicatum, Coniella granati and Aspergillus niger. Fruit pre- and postharvest losses is due to bacterial and fungal diseases [4]. Demand for fruit decreases if physical disorder such as rind cracking, chilling injury and husk scald are visually seen on the fruit [5]. Nearly 40% of loss due to improper packaging and storage is observed in India among people doing business with pomegranate

[6]. In India there is lot of prominence given to grow pomegranate as it is nutritious and is in good demand in countries outside India, hence aiding economic growth [Singh 2023]. In order to improve yield in growth of pomegranate fruit product it is required quality control growth of the fruit by pest management and monitoring the growth under various environmental conditions. One of the newest methods is to use machine learning techniques that process the images captured and processes these images captured at various stages in plant growth, flower growth and fruit growth. By continuous monitoring progressing in growth pattern of plant, leaves, flowers and fruit there can be immediate remedies adopted to prevent the damage to the crop. Several studies on use of Artificial Intelligence and Machine Learning methods are reported in literature for development of automated algorithms for estimating diseases in the fruit at early stages. Few of the methods that have been widely used are based on random forest model by Naseer et al [7] and Nirgude et al. [8] with accuracy of 98% and 96.53 % as reported in literature. CNN based model (ResNet50) by Nirgude et al. [9] reports identification of 5 diseases with accuracy of 97.92%. Vasumathi et al [10] have used hybrid CNN LSTM model to identify four different diseases with accuracy of 97.21%. The work carried out by [11] have proposed model PomeNetV2 CNN to detect 4 diseases such as: Alternaria, Anthracnose, Bacterial Blight, Cercospora and Healthy. In their work 5099 images are considered for processing and have demonstrated 99.02% accuracy in identifying the diseases with 75 epochs of training. The model requires six stages of Convolution layer and max pooling layer with one flattening layer at the output and two preprocessing layers at the input. For faster processing of data and providing inferences to the farmer, there is a requirement for reducing the computation complexity in the CNN model. In this work, an improvised method is developed that combines wavelet features for training CNN model.

## 2. Pomegranate disease and control mechanism

Figure 1 presents the four types of disease considered in this work for development of improvised methods to detect and classify the diseases. The data sets from [12] are used in this work.



Fig. 1 Pomegranate disease types

Table 1 presents the diseases and the control mechanism to prevent the spread of the disease [13].

**Table 1: Disease and control mechanism in pomegranate disease**

Disease	Control mechanism
Cercospora Fruit Spot ( <i>Cercospora</i> sp.) - The affected fruits showed small irregular black spots, which later on coalesce, into big spots.	The diseased fruits should be collected and destroyed. Two to three spraying at 15 days interval of Dithane M-45 or Captan @ 2.5 g in one litre of water after fruit formation gives good control of the disease.
Fruit Rot ( <i>Aspergillus foetidus</i> )- The symptoms are in the form of round black spots on the fruit and petiole. The disease starts from calyx end and gradually the entire fruit shows black spots. The fruit further rots emitting a foul odour.	The disease can be controlled by spraying of Bavistin (0.5%), Dithane M-45 (0.25%) or Dithane Z-78 (0.25%) at an interval of 10-15 days from the onset of flowering.
Leaf Spot or Blight ( <i>Colletotrichum gloesporioides</i> ; <i>Pseudocercospora punicae</i> ; <i>Curvularia lunata</i> and <i>Cercospora punicae</i> )- The disease is characterized by appearance of small, irregular and water-soaked spots on leaves. Affected leaves fall off.	Spraying of Topsin-M (0.1%), Sulfex (0.03%), Difolatan (0.2%) or Dithane M-45 (0.3%) at 15 days interval gives good control of the disease.
Alternaria Fruit Spot ( <i>Alternaria alternata</i> )- Small reddish brown circular spots appear on the fruits. As the disease advances these spots, coalesce to form larger patches and the fruits start rotting. The arils get affected which become pale and become unfit for consumption.	All the affected fruits should be collected and destroyed. Spraying Dithane M 45 (0.25%) or Captaf (0.25%) effectively controls the disease

Pomegranate disease is mainly identified in tropical and subtropical regions where the fruit borer population is more, because of favourable environmental condition for borers. These bacterial and fungus infect the fruits in several stages [14]. In earlier days, health monitoring of plants is very difficult and the farmers fail to identify the diseases of plants in their early stages. Hence automation is very much needed in the field of identification of diseases very quickly. The information of the preventive measures is very much needed in order to overcome the infection. The system has been developed using image processing; hence this might help the farmers to get high yield indirectly.

### 3. Proposed Method

Figure 2 presents the block diagram of the proposed model, the input image is pre-processed (techniques such as contrast enhancement, histogram equalization and normalization are carried out) and the pre-processed image is transformed into wavelet domain (level-1) using biorthogonal 4.4 wavelet filter (Discrete Wavelet Transform (DWT)). The three high pass sub bands denoted as LH, HL and HH are quantized and thresholded to retain the localised edge information along the vertical, horizontal and diagonal directions. The LL low pass sub band is processed to remove high frequency noise. Wavelet subbands after post processing are combined and Inverse DWT is carried out to get back the input image without noise and with localized and significant features. Three stages of CNN module (each stage comprising of Convolution Layer (CL) and Max Pooling Layer (MPL)) are trained to learn and detect the specific features in the image obtained from IDWT. At each stage of Convolutional Neural Network (CNN) the dimensions of image are reduced and at the third stage the 2D output is flattened to 1D data. Feed Forward Fully Connected Neural Network (FCNN) model is used to process the 1D feature for classification into 6 classes of diseases (four diseases listed in Table 1). The Disease Classifier (DC) model is developed to infer the diseases into any four of them. Control Module (CM) is developed to generate or recommend suitable control mechanisms that can be adopted to control the spread of disease or to eliminate the disease at the early stage. The CM block is developed considering the details presented in Table 1.

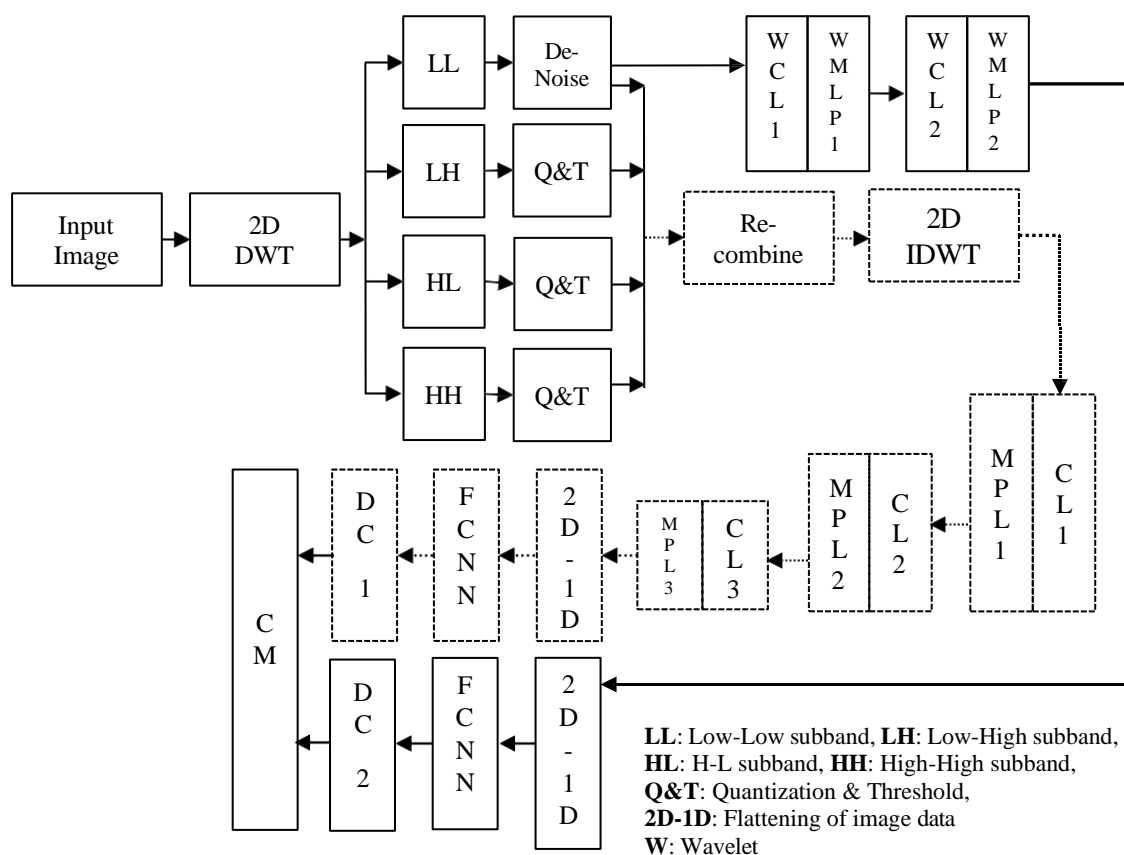


**Figure 2: Proposed disease detection, classification and inference model**

In Figure 2 two models are presented: 1. DWT with CNN (dotted line blocks) and 2. LL band with CNN (solid line blocks). The DWT with CNN model performs denoising and filtering in the wavelet domain, and the DWT subbands are combined together and inverse DWT is carried out and the image is further processed using three state CNN model {Stage 1: CL<sub>1</sub>, MPL<sub>1</sub>, Stage 2: CL<sub>2</sub>, MPL<sub>2</sub>, Stage 3: CL<sub>3</sub>, MPL<sub>3</sub>}. Further, the output of 3<sup>rd</sup> stage CNN is flattened into 1D and is processed by FCNN to perform detection and classification. In the LL band with CNN model, the LL band of DWT is denoised and two stages of CNN model {Stage 1: WCL<sub>1</sub>, WMPL<sub>1</sub>, Stage 2: WCL<sub>2</sub>, WMPL<sub>2</sub>} is used, and the output of stage 2 is flattened to 1D and is processed by the FCNN module to perform detection and classification of diseases. The output of DC<sub>1</sub> and DC<sub>2</sub> are used for control mechanism as well as to compare the results. It is advantageous to process wavelet sub band and train the CNN model for classification. The CNN model trained with wavelet sub bands will be able to learn non-redundant features as wavelet transform groups the features into four subbands, this will reduce computation complexity as the CNN model is trained to learn essential features. Wavelet subbands capture both spatial and temporal features, thus enabling learning capability of CNN model that considers both information [15]. The subbands generated is processed for denoising that is carried out in wavelet domain that will improve noise from the input and also classification accuracy of CNN model. With four subbands in every level of wavelet decomposition, localization of edge features and pixel transition obtained which will directly enhance features that can be trained to be classified by the CNN model to differentiate between different classes based on these localized features. With dimensionality reduction in the wavelet domain, computation complexity for CNN to operate is also minimized [16]. DWT subbands for training CNN model is much suitable when there are limited data sets, and with localization of sub bands CNN model can be trained to capture these features and enhance classification accuracy. There also limitations in training CNN model with DWT subbands. In the process of decomposition, information that are more relevant in spatial domain may be lost in the wavelet domain. Selection of appropriate wavelet filter will minimise



loss of information. With DWT module, number of stages in the classification model will add additional delay and increase complexity. There need to be a trade-off of delay and accuracy, suitable fast transform algorithms need to be considered. Conventional CNN models are developed to operate on images represented in spatial domain, with DWT sub bands comprising of wavelet features, CNN model need to be customized to process these sub bands. In this work, two methods are proposed: 1> Processing of reconstructed images after DWT by the CNN model, 2> Processing of denoised LL sub band by CNN model. In method 1, by transforming the input image into wavelet sub bands, noise removed in the wavelet domain by performing Q&T and the significant edges or features or frequencies that are dominant are retained in the wavelet domain. Inverse DWT is performed to reconstruct the image without noise and with dominant features. In method 2, the LL sub band that captures the maximum information is considered to train the CNN model. As the dimension of LL sub band is half of the input image size the computation complexity of CNN model is reduced by half. The output of both methods is processed by the DC1 and DC2 model and the decisions are combined to generate inferences in the CM as per the details provided in Table 1.

#### 4. Experimental work and results

The input image is processed to compute DWT sub bands as expressed in Eq. (1), where the input image  $I(x,y)$  is convolved with scaling ( $\phi$ ) and wavelet ( $\psi$ ) function to obtain the four sub bands denoted as LL, LH, HL and HH. The sub bands  $LL(m, n)$  represent the low pass sub band with image size of  $m \times n$ .

$$LL(m, n) = \sum_x \sum_y I(x, y) \phi(x - 2m) \phi(y - 2n) \quad (1a)$$

$$LH(m, n) = \sum_x \sum_y I(x, y) \phi(x - 2m) \psi(y - 2n) \quad (1b)$$

$$HL(m, n) = \sum_x \sum_y I(x, y) \psi(x - 2m) \phi(y - 2n) \quad (1c)$$

$$HH(m, n) = \sum_x \sum_y I(x, y) \psi(x - 2m) \psi(y - 2n) \quad (1d)$$

The wavelet filter that is considered in this work is 'db4' with scaling filter Coefficients  $h = [0.48296, 0.8365, 0.22414, -0.12941, -0.0968, 0.02733, 0.01994, -0.00485]$  and the wavelet function is given as in Eq. (2),

$$g[n] = (-1)^n h[L-1-n], n \text{ is the filter order } (2)$$

Fourier Transform is computed to determine the global frequency distribution for the DWT bands as in Eq. (3), where  $u, v$  represents frequency indices in the horizontal and vertical directions.

$$F_{LL}(u, v) = \sum_x \sum_y LL(m, n) e^{-j2\pi \frac{ux}{M} + \frac{vy}{N}} \quad (3a)$$

$$F_{LH}(u, v) = \sum_x \sum_y LH(m, n) e^{-j2\pi \frac{ux}{M} + \frac{vy}{N}} \quad (3b)$$

$$F_{HL}(u, v) = \sum_x \sum_y HL(m, n) e^{-j2\pi \frac{ux}{M} + \frac{vy}{N}} \quad (3c)$$

$$F_{HH}(u, v) = \sum_x \sum_y HH(m, n) e^{-j2\pi \frac{ux}{M} + \frac{vy}{N}} \quad (3d)$$

The advantages of computing FFT on DWT sub bands helps in analysis of frequency content in each of the four sub bands and also provides information on global frequency spectrum in addition to the localized frequency information in the time-frequency analysis by DWT. Feature extracted with DWT sub bands provide information of localized variations and by computing FFT on DWT sub bands provide information on variations in frequency patterns [17].

Figure 3 presents the DWT output of pomegranate image with five diseases considered, row 1 in the figure presents the five diseases and corresponding location of the disease on the fruit. In row 2 of the figure the LL sub band is represented, the visual information as compared with the original image (row 1) there is less difference, however the size of the LL sub band is reduced by half. The images in row 3 to row 5 represent the Vertical (LH), Horizontal (HL) and Diagonal (HH) sub bands. The high

frequency sub bands capture the edge information along the vertical, horizontal and diagonal directions as seen in the figure.

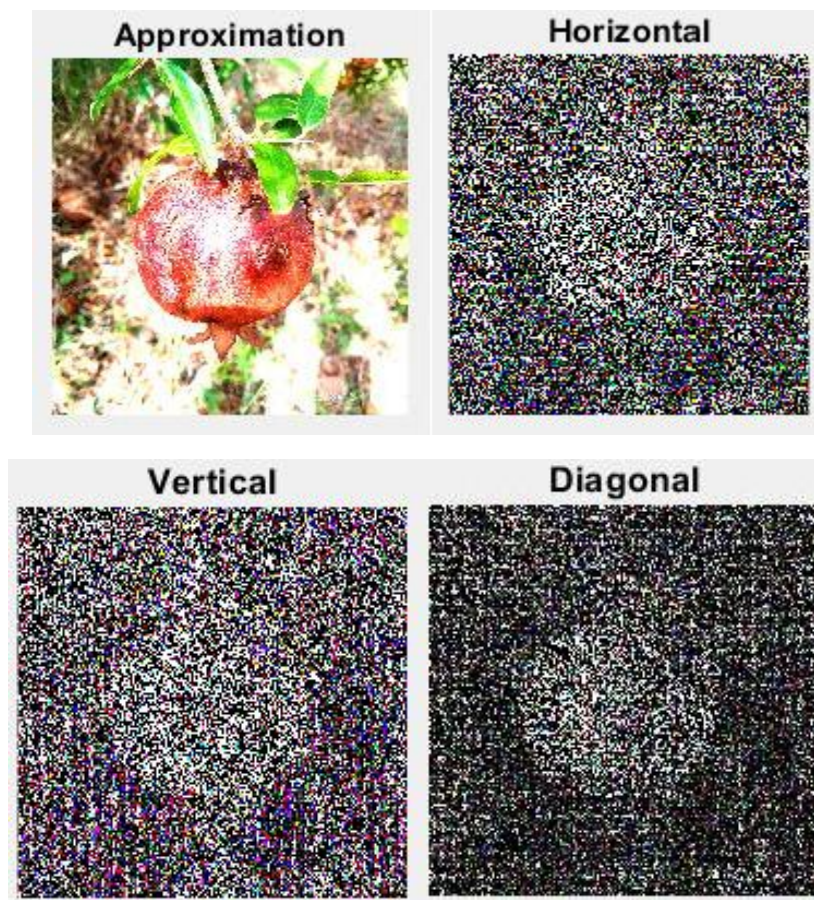


**Figure 3: Wavelet sub band of pomegranate**

Figure 4 presents the energy distribution in the original image and the wavelet sub bands. The energy distribution in both time and frequency domain are computed and presented. The first row in Figure 4a is the energy distribution in original image both in time and frequency (computed using FFT). The second row in Figure 4a is the time domain and frequency domain energy distribution of LL sub band. The frequency domain distribution in the original image is concentrated in the middle of the graph indicated and the size of the image is 443 x 271. In the wavelet domain (LL sub band), the energy in the frequency domain is similar to that of original image with dimensionality reduced to 225 x 139.

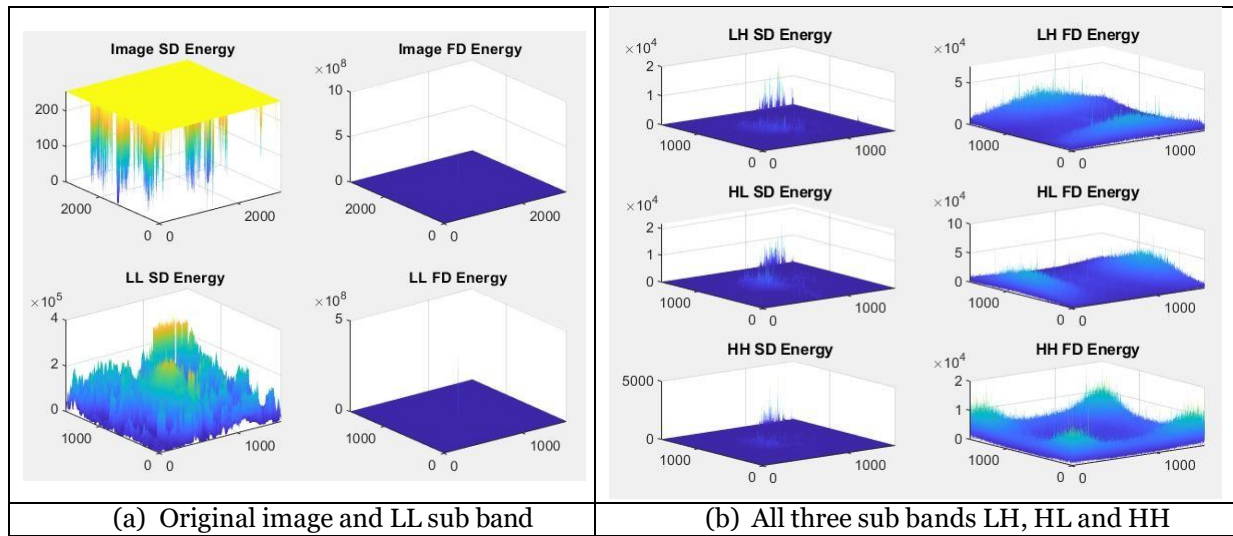


**Figure 4: Comparing energy distribution in time domain and wavelet domain using FFT**

In Figure 4b, localised energy of the wavelet sub bands (LH, HL and HH) is compared with the global energy distribution. It is observed that there is redundancy in energy distribution as observed in the global energy distribution plots. In the localised energy distribution plots, the energy is concentrated in localised areas considering the vertical, horizontal and diagonal edges in the input image. Figure 5 presents the denoised images and corresponding energy distribution in all the four wavelet sub bands. In this work denoising is carried out by using Gaussian filter and the wavelet sub bands are convolved with Gaussian filter  $G(I, j)$  to generate image  $LH'(x, y)$  from input image  $LH(m, n)$  as in Eq. (4),

$$LH'(m, n) = \sum_{i=-kc}^{kc} \sum_{j=-kc}^{kc} LH(m + i, n + j) \cdot G(i, j) \quad (4)$$

For a filter size is  $k \times k$  ( $k$  is set to 3 or 5 or 7),  $kc$  is the centre point of the filter  $k \times k$ , and standard deviation  $\sigma$  (this is set between 0.5 to 1, considering low level noise), the Gaussian filter  $G(I, j)$  is given as in Eq. (5),

$$G(I, j) = \frac{1}{2\pi\sigma^2} \exp\left(-\frac{((i-kc)^2 + (j-kc)^2)}{2\sigma^2}\right), \text{ where } kc = \left\lfloor \frac{k}{2} \right\rfloor \quad (5)$$

Considering Eq. (4) and Eq. (5) denoising is carried out on all the other two sub bands.

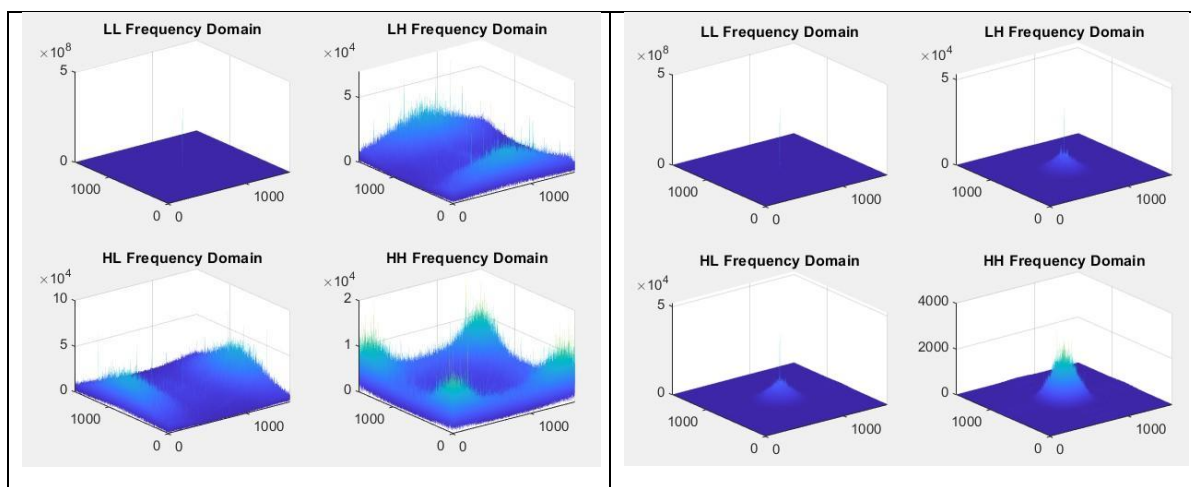


**Figure 5: Frequency distribution before and after denoising**



Denoising of LH, HL and HH sub band is carried out by computing the gradient operation using Sobel operator and then performing gaussian filtering operation. The LH, HL and HH sub band is quantized and thresholded (Q&T) by setting the  $\sigma$  value between 1.0 to 2.0. In Figure 5 it I observed that by denoising and Q&T of the sub bands the features in the frequency band are localized and these features are extracted for training the convolution neural network model. The convolution model further extracts the features that are localized in the input image ( $X \in \mathbb{R}^{H \times W \times C}$ ) with convolution kernels or filters of height (H), width (W) and channels (C) to obtain an output feature map ( $F \in \mathbb{R}^{H' \times W' \times K}$ ) with k number of filters.

The convolution operation is expressed as in Eq. (6), where fh and fw are filter size and Xc is the input image (in this work it is LL(m, n) and other sub bands),  $W_{k,c}$  is the filter weights and (I, j) represent the filter positions for feature map of the input images. Activation function ReLU is used after convolution processing, further followed with maximum pooling (MPL) operation [18] - [20].

$$F_k(I, j) = \left( \sum_{c=1}^C \sum_{u=1}^{f_h} \sum_{v=1}^{f_w} X(i+u-1, j+v-1) \cdot W_{k,c}(u, v) + b_k \right) \quad (6)$$

The MPL operation is expressed mathematically as in Eq. (7),

$$P_k(i, j) = \max [F_k(i.s + u, j.s + v)], \text{ with matrix window size of } p = 2. \quad (7)$$

As discussed in Figure 2, CNN model is repeated twice if operated on wavelet features. The denoised image in wavelet domain and reconstructed image after DWT is processed by 3 stages of CNN model. After CNN 2D to 1D is carried out and FCNN model is used to classify the diseases. The final layer of CNN is the fully connected neural network model. In this work the neural network architecture is designed to have an input layer of 22 x 1 vectors. Figure 6 presents the fully connected layer structure. The hidden layer 1 outputs are denoted as {a11, a21, a31 ..., as11}. The intermediate output of each neuron of the intermediate layer is denoted as {n11, n21, n31... ns11}. Similarly, the intermediate and output of second layer is denoted as n2s2 and a2s2. The network activation function for all the hidden layers and output layer is selected to be tansig or purelin. The intermediate output ( $n_m^1$ ) of hidden layer 1 is mathematically represented as in Eq. (8), and the output of hidden layer is demoted as in Eq. (9).

$$n_m^1 = \sum_{l=1}^{22} E_l w_{m,l}^1 + b_m^1 \quad (8)$$

$$a_m^1 = \text{tansig}(n_m^1), m=(1,2,3,4...15) \quad (9)$$

The weights are denoted by  $w_{m,l}$  and the bias is denoted as  $b_m^1$ . For the first hidden layer, if the number of neurons is set to N, the number of weights is 22N. As every neuron will have 22 weights as there are 22 energy levels. The number of biases in the hidden layer will be m. Similarly, all other hidden layer outputs are denoted and represented as  $n_k^p$ , where k represents number of neurons in the hidden layer p. Eq. (10) and Eq. (11) presents the intermediate output and final output of hidden layer 2. Table 2 summarizes the configuration of CNN model.

$$n_k^2 = \sum_{l=1}^{15} a_l^1 w_{k,l}^2 + b_k^2 \quad (10)$$

$$a_k^2 = \text{tansig}(n_k^2), n = (1,2,3,...40) \quad (11)$$

**Table 2: Summarizes the size of frames for proposed CNN Model**

Input	Size(N*N)	Frames
	N*N	1
CL1	(N-1)*(N-1)	4
MP1	[(N-1)/2]*[(N-1)/2]	4
CL2	[(N-3)/2]*[(N-3)/2]	16
MP2	[(N-3)/4]*[(N-3)/4]	16
CL3	[(N-7)/4]*[(N-7)/4]	16*4
MP3	[(N-7)/8]*[(N-7)/8]	16*4
OL1	[(N-7)/8]*[(N-7)/8]	8*4



OL2	$[(N-7)/8]*[(N-7)/8]$	$8*2$
FCNN	1 D Network	

In proposed architecture the Input data is processed by 3 stages of CL + MPL module & one layer of Fully Connected Neural Network Layer (FCNN). The CL module has 4 filters to extract features in all directions of orthogonality. The 1<sup>st</sup> stage generates 128 x 128 from 256 x 256 size input image. The 2<sup>nd</sup> stage & 3<sup>rd</sup> stage together generate image with feature map of size 16 x 16 x 4. The flattening modules converts 2D (16 x 16 x 4) data to 1D Vector of size (1024 x 1). The FCNN Layer (shown in Figure 6) process 1024 vectors using 4 stages of Neural Network module to generate M Outputs (M=3, to classify 5 diseases and 1 image without disease).

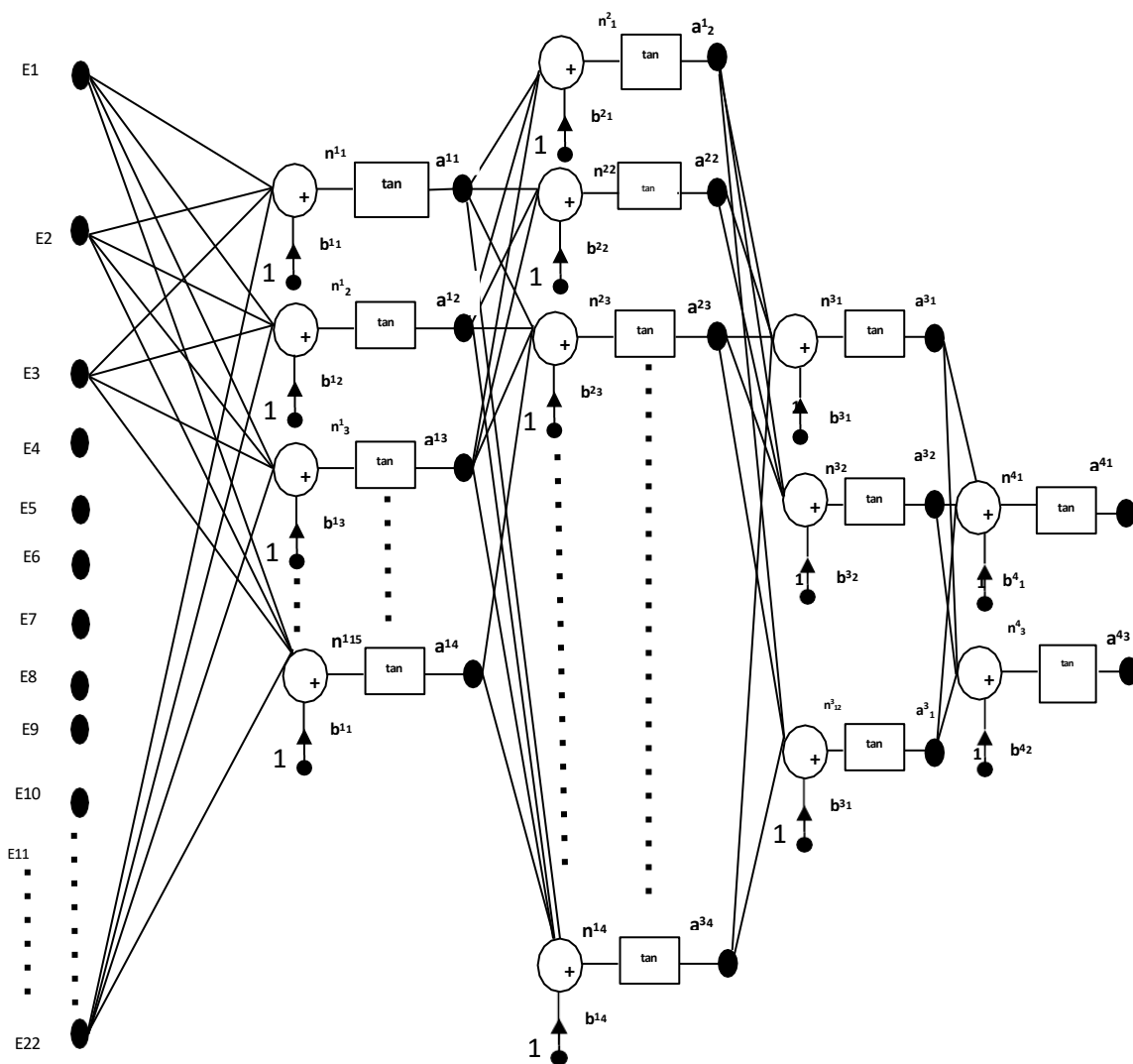


**Figure 6: Fully connected neural network model for CNN**

CNN model is proposed in this work is modelled in MATLAB and the model is trained with data set comprising of 2556 images of four groups of diseases. From the total dataset 30% of the dataset is assigned for test and validation process. The ConvNets model is used as they generate spatially correlated results. ConvNets have three layers, max-pooling layers and fully connected layer. The neurons in each layer are organized in 3D matrix and is processed using 3D processing unit to generate 3D output data. The function in MATLAB for ConvNets is defined as in Figure 7. The model is trained

and trained model is validated with the datasets to determine the accuracy of classification. The results obtained are discussed in next section.





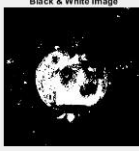
<p>DWT is used for denoising with 'db4' filter. DWT feature is processed using CNN model.</p> <pre> layers = [     image Input Layer ([n n 1])     convolution 2d Layer (5,20)     relu Layer     max Pooling 2d Layer (2, Stride=2)     fully Connected Layer (10)     soft max Layer]; %% the number of layers is repeated twice if DWT features are processed or it is repeated thrice if operated on reconstructed image. </pre>	<pre> options = training Options ("sgdm", ...     Initial Learn Rate=0.1, ...     Max Epochs=2, ...     Plots="training-progress"); net = train Network (imds Train, layers, options); Initial Learn Rate=0.01 Max Epochs=4 YPred = classify (net, imds Validation); Y Validation = imds Validation. Labels; accuracy = sum (Y Pred == Y Validation) / numel (Y Validation); </pre>
--	---

**Figure 7: MATLAB model for classification of pomegranate disease**

In MATLAB there are several CNN models of which YOLO model is very much and reported in literature. For detection of plant diseases YOLO model is not recommended as there are four types pomegranate fruit diseases and YOLO is best suitable for classification of more than 20 classes. A simplified YOLO model is reported in [21], and the complexity of training the model is simplified and compared. From the studies reported in [21] Tiny- YOLOV4 model that uses Darknet-19 backbone architecture occupies less than 33.4 MB size, can operate at a speed of 220 frames per second and has higher mean average precision (mAP) of 99.9%. The limitations of this model is the number of data sets if limited will result in reduce accuracy of classification. To overcome this limitations and to ensure higher processing speed, YOLOV4 model is combined with DWT so as to process the features to achieve higher classifications.

## 5. Discussion

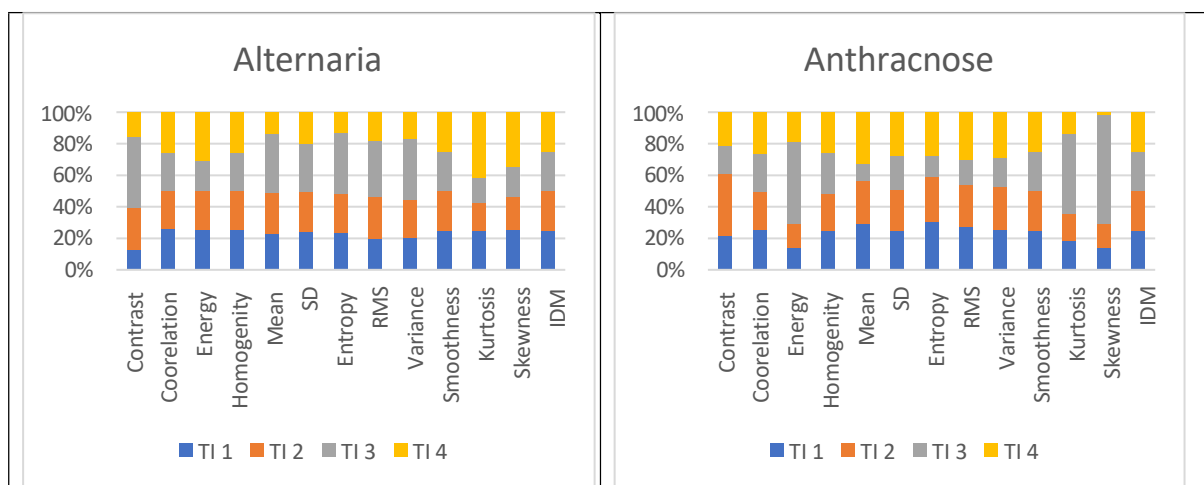
The MATLAB model developed considers all the four datasets and the features that are extracted considering three aspects: 1> Background image without disease infected area, 2> Disease infected area or region and 3> Disease infected region with background area. These three regions are termed as clusters 1, 2 and 3. Features from these clusters are identified and we consider 13 features: Contrast, correlation, energy, homogeneity, entropy, kurtosis, skewness, mean, RMS, variance, standard deviation, smoothness and IMD. Of the 13 features only seven are considered for analysis and disease detection. Figure 8 presents the details of four disease with input image in column 2, and three clusters in column 3, 4 and 5. Column 1 presents the details of infected area of corresponding disease. From each of the clusters, seven features are identified and used for disease classification. The DWT features are also combined with these features and are used as training data set for the CNN model discussed.

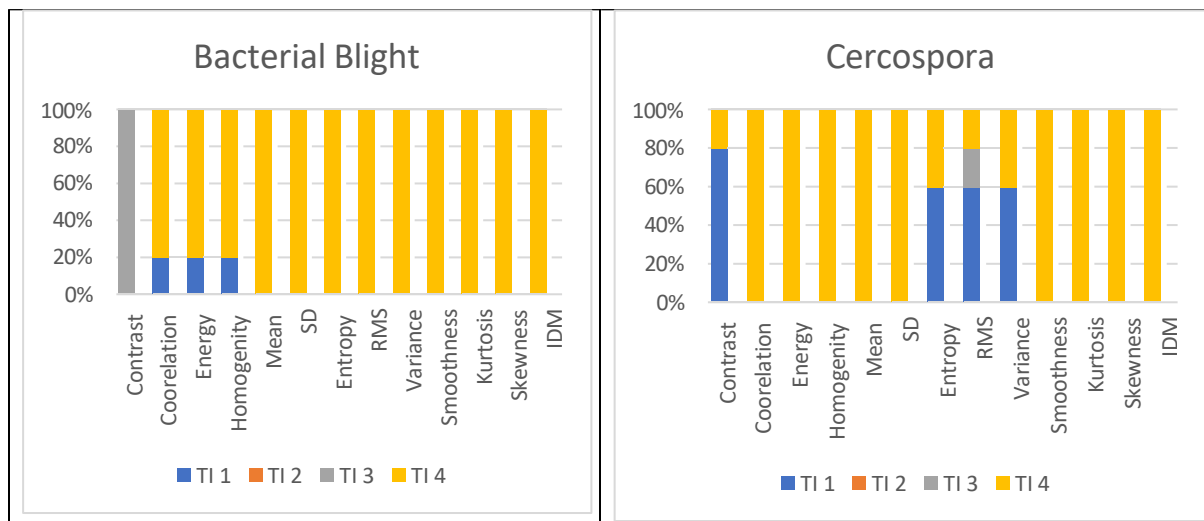
Alternaria					
Affected Area %	Input image	Feature 1	Feature 2	Feature 3	B&W Image
15.0956					
Anthracnose					
Affected Area %	Input image	Feature 1	Feature 2	Feature 3	B&W Image

58.8997					
Bacterial Blight					
Affected Area %	Input image	Feature 1	Feature 2	Feature 3	B&W Image
43.0364					
Cercospora					
Affected Area %	Input image	Feature 1	Feature 2	Feature 3	B&W Image
15.0124					
Healthy					
Affected Area %	Input image	Feature 1	Feature 2	Feature 3	B&W Image
15.0124					

**Figure 8: Clusters considered for feature detection for classification**

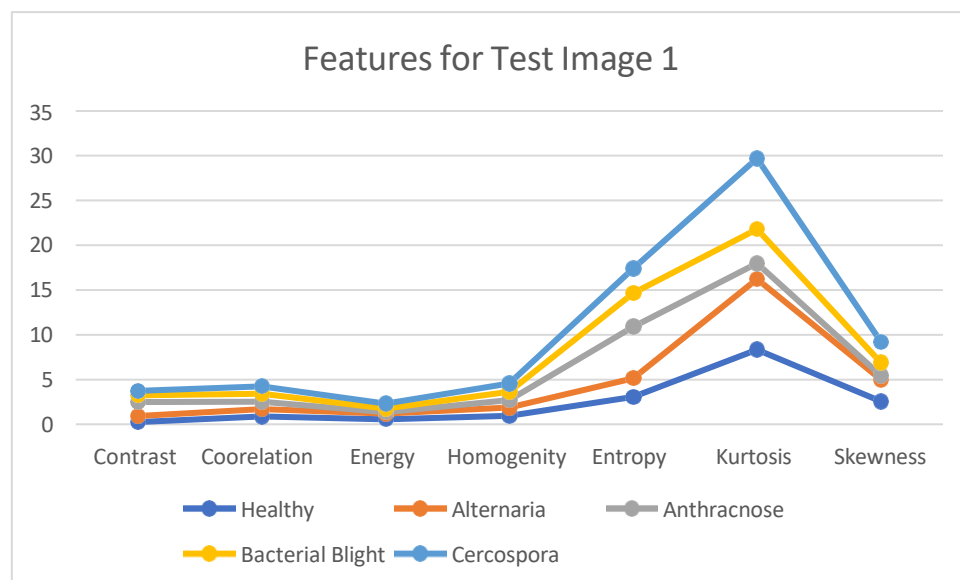
Figure 9 presents the 13 features for four test images and the variation are plotted in percentages. It is identified that all the features for all four diseases vary within a permissible band and does not infringe or have random changes which will impact the classification process.





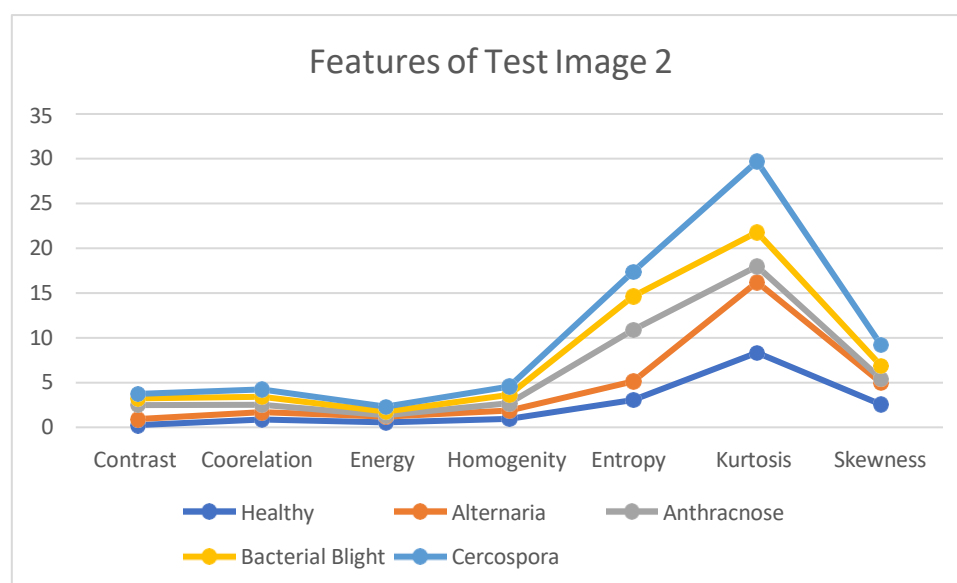
**Figure 9: Feature distribution observed with percentage changes**

Figure 10 presents the feature distribution comparing four diseases considering two test images. It is observed that the pomegranate fruit which is healthy, the feature is at the bottom of the curve (blue color line) and there is a significant difference in variations compared with all other images for four diseases. Comparing the line distribution, the features homogeneity, entropy, kurtosis and skewness are distinct and are the major factors that support detection and classification process.



**a. Feature distribution for test image 1**





b. Feature distribution for test image 2

**Figure 10: Comparison of feature variations for detection and classification for all four diseases**

Considering seven features, it is observed that the proposed method has significant number of redundant features that can aid in accurate classification of pomegranate disease. The proposed model “DWT with TinyYOLOV4” is modelled in MATLAB and trained. As discussed, two methods are proposed: 1> CNN model operating on DWT sub bands, 2> CNN with denoised & reconstructed image using DWT. Both of these methods are trained with pomegranate data sets and is validated considering 20% of the total data set available. The initial parameters for training are set with a batch size of 256 images, initial training rate of 0.001, decay of 0.004 and training steps of 5000. Total number of images are 2556 of which 2048 images are set for training and 508 images are considered for testing. The trained model is validated and is compared with previous methods. The YOLOV4 model is used as well for comparison, as the number of data sets are limited and less than 1000 with four classes the Mean Average Precision (mAP) is found to be 98.88%. Further the mAP of the proposed methods are also listed in Table 4. The Tiny YOLOV4 algorithm reported in [21] is also considered for comparison. From the comparison results it is found that both the methods proposed in this work are superior to the existing methods.

**Table 4 :Accuracy of proposed model**

Model	Mean average precision
DWT with Tiny YOLOV4 (method 1)	99.34%
DWT with Tiny YOLOV4 (method 2)	99.26%
YOLOV4	98.47%
Tiny-YoloV4 (for pomegranate) [21]	97.11%
MobileNetV2-YoloV3 (for pomegranate) [21]	97.29%
Yolo-Fastest (for pomegranate) [21]	96.61%

Table 5 compares the performances of all three methods considered in this work, considering individual images. The mAP of all three methods is reported and the method 1 and method 2 have been recommended for pomegranate fruit disease classification. Method 1 is able to achieve higher precision

in classification compared with YOLOV4 algorithm. Method 2 is also on par with method 1 and hence the inference logic model presented in this work, considers both the methods and recommends the control mechanism to the farmer as per the details provided in Table 1.

**Table 5: mAP of proposed model for four diseases**

Model	Alternaria	Anthracnose	Bacterial Blight	Cercospora	Healthy
DWT with YOLOV4 (method 1)	98.61%	99.01%	99.23%	99.86%	99.99%
DWT with YOLOV4 (method 2)	98.43%	98.98%	99.21%	99.72%	99.99%
YOLOV4	97%	98.2%	98.89%	99.1%	99.2%

Pomegranate disease “Cercospora” is detected with higher precision accuracy of 99.86%. As the algorithm considers the DWT features and trains the CNN model with DWT features the limitation in limited number of data sets is addressed. The validation process results indicates that there is 2% variation in precision accuracy as compared with training data set classification.

## 6. Conclusion

Pomegranate disease is detected and classified using two methods that combines the DWT features with CNN model for training. The proposed TinyYOLOV4 is trained with two sets of input data: DWT sub bands and denoised images. Both of these methods have been trained with four types of Pomegranate diseases of which one dataset is healthy Pomegranate. The DWT sub bands capture the frequency information and the denoising algorithm localizes the high frequency components and the denoised sub bands are reconstructed for further processing. In the second method, the DWT sub bands are used to train the CNN model that reduces computation complexity and is faster the CNN model process images that are 50% reduced in size as compared with input image. The mean average precision in disease classification is 99.34% and the proposed method has achieved 4% improvement over existing methods reported in literature. Further the results of two methods are combined to improvise classification accuracy and also to provide inferences in terms of control mechanisms. The proposed model is suitable for real time data processing as the computation complexity is addressed by operating on DWT features.

## References

- [1] Chowdhary, M. E. H., Rahman, T., & Khandakar, A. (2021). Automatic and reliable leaf disease detection using deep learning technique. *Agri Engineering*, 3(2), 294-312. [https://doi.org/\[DOI\]](https://doi.org/[DOI])
- [2] Chakali, R. (2020). Effective pomegranate plant leaf disease detection using deep learning. *International Journal of Circuit, Computing and Networking*.
- [3] Zhang, H., Xie, F., Liu, S., Liu, X., & Wang, J. (2022). Real-time detection of plant disease using deep learning and mobile phone-based hyperspectral imaging. *Journal of Applied Remote Sensing*, 16(1), 016510. [https://doi.org/\[DOI\]](https://doi.org/[DOI])
- [4] Tziros, N., & Tzavella-Klonari, K. (2008). Mondal et al. (2012).
- [5] Caleb, O. J., et al. (2012). Modified atmosphere packaging of pomegranate fruit and arils: A review. *Food Bioprocess Technology*.
- [6] Munhuweyi, K., Lennox, C. L., Meitz-Hopkins, J. C., Caleb, O. J., & Opara, U. L. (2016). Major diseases of pomegranate (*Punica granatum* L.), their causes, and management—A review. *Scientia Horticulturae*, 211, 126-139. [https://doi.org/\[DOI\]](https://doi.org/[DOI])
- [7] Naseer, A., Amjad, M., Raza, A., Munir, K., Abdelsamee, N., & Alohal, M. (2024). A novel transfer learning approach for detection of pomegranates growth stages. *IEEE Access*. <https://doi.org/10.1109/ACCESS.2024.3365356>

- [8] Nirgude, V., & Rath, S. (2021). A robust deep learning approach to enhance the accuracy of pomegranate fruit disease detection under real field condition. *Journal of Experimental Biology and Agricultural Sciences*, 9(6), 863-870.
- [9] Nirgude, V., & Rath, S. (2024). i-Pom Diagnoser: A real-time pomegranate disease management system. *Indian Journal of Science and Technology*, 17(14), 1391-1401. <https://doi.org/10.17485/IJST/v17i14.57>
- [10] Vasumathi, M. T., & Kamarasan, M. (2021). An effective pomegranate fruit classification based on CNN-LSTM deep learning models. *Indian Journal of Science and Technology*, 14(16), 1310-1319.
- [11] Pakruddin, B., & Hemavathy, R. (2024). Development of a pomegranate fruit disease detection and classification model using deep learning. *Indian Journal of Agricultural Research*, 58, 1121-1130. <https://doi.org/10.18805/IJARE.A-6281>
- [12] Pakruddin, B., & Hemavathy, R. (2023). Pomegranate fruit diseases dataset for deep learning models. *Mendeley Data*, V1. <https://doi.org/10.17632/b6s2rkpmvh.1>
- [13] National Horticulture Board. (n.d.). *Pomegranate cultivation*. Retrieved from [www.nhb.gov.in/pdf/fruits/pomegranate/pom002.pdf](http://www.nhb.gov.in/pdf/fruits/pomegranate/pom002.pdf)
- [14] Sharath, D. M., et al. (2020). *Proceedings of the Fourth International Conference on Trends in Electronics and Informatics (ICOEI 2020)*. IEEE Xplore. ISBN: 978-1-7281-5518-0
- [15] Tabassum, F., Islam, M. I., Khan, R. T., & Amin, M. R. (2022). Human face recognition with combination of DWT and machine learning. *Journal of King Saud University - Computer and Information Sciences*, 34(3), 546-556. [https://doi.org/\[DOI\]](https://doi.org/[DOI])
- [16] Xie, Y., & Zhang, T. (2017). Feature extraction based on DWT and CNN for rotating machinery fault diagnosis. *2017 29th Chinese Control and Decision Conference (CCDC)*, 3861-3866. <https://doi.org/10.1109/CCDC.2017.7979176>
- [17] Yang, X., Gong, J., Wu, L., Yang, Z., Shi, Y., & Nie, F. (2023). Reference-free low-light image enhancement by associating hierarchical wavelet representations. *Expert Systems with Applications*, 213, 118920. [https://doi.org/\[DOI\]](https://doi.org/[DOI])
- [18] Redmon, J., & Farhadi, A. (2018). YOLOv3: An incremental improvement. *arXiv:1804.02767[cs.CV]*. Retrieved from <https://arxiv.org/abs/1804.02767>
- [19] Wong, A., Famuori, M., Shafiee, M. J., Li, F., Chwyl, B., & Chung, J. (2019). YOLO nano: A highly compact You Only Look Once convolutional neural network for object detection. *arXiv*. Retrieved from <https://arxiv.org/abs/>
- [20] Jadhav, S. B., Udipi, V. R., & Patil, S. B. (2021). Identification of plant diseases using convolutional neural networks. *International Journal of Information Technology*, 13, 2461-2470. <https://doi.org/10.1007/s41870-020-00437-5>
- [21] Khatawkar, S., Jadhav, S., Sapate, S., Patil, P., & Shinde, A. (2023). Disease detection on pomegranate fruits using machine learning approach. *AIP Conference Proceedings*, 2717(1), 020004. <https://doi.org/10.1063/5.0130455>
- [22] Mitkal, P. S., & Jagadale, A. (2023). Grading of pomegranate fruit using CNN. *Age*, 3(2).
- [23] Thakur, S., Malik, D., Kukreja, V., Sharma, R., Yadav, R., & Joshi, K. (2023, September). Multi-stage classification of pomegranate anthracnose disease severity levels with CNN and SVM. In *2023 4th International Conference on Smart Electronics and Communication (ICOSEC)*, IEEE. pp. 1117-1121.